

Role of three-nucleon forces in neutron-rich nuclei beyond ^{132}Sn

Luigi Coraggio

Istituto Nazionale di Fisica Nucleare - Sezione di Napoli

June, 6th 2014



- ▶ A. Covello (University of Naples and INFN)
- ▶ A. Gargano (INFN)
- ▶ N. Itaco (University of Naples and INFN)
- ▶ L. C. (INFN)

Motivations

- ▶ What is the **balance** between the role of **2NF** and **3NF**?
- ▶ Neutron-rich nuclei above ^{132}Sn provide a valid laboratory to study this topic
- ▶ To investigate the influence of **three-body correlations** on the **monopole components** of the shell-model hamiltonian

Our framework: the realistic shell model

- ▶ **First step:** choose a realistic nucleon-nucleon potential and renormalize short-range correlations
- ▶ **Second step:** choose a convenient model space
- ▶ **Third step:** derive an effective shell-model hamiltonian H_{eff} by way of the many-body perturbation theory
- ▶ **Fourth step:** diagonalize the shell-model hamiltonian in the chosen model space

L. C., A. Covello, A. Gargano, N. Itaco, and T. T. S. Kuo, Prog. Part. Nucl. Phys. 62 (2009) 135



The shell-model effective hamiltonian

A versatile way to derive H_{eff} is the time-dependent perturbative approach as developed by Kuo and his co-workers in the 1970s (see *T. T. S. Kuo and E. Osnes, Lecture Notes in Physics vol. 364 (1990)*)

The shell-model effective hamiltonian

A versatile way to derive H_{eff} is the time-dependent perturbative approach as developed by Kuo and his co-workers in the 1970s (see *T. T. S. Kuo and E. Osnes, Lecture Notes in Physics vol. 364 (1990)*)

In this approach the effective hamiltonian H_{eff} is expressed as

$$H_{\text{eff}} = \hat{Q} - \hat{Q}' \int \hat{Q} + \hat{Q}' \int \hat{Q} \int \hat{Q} - \hat{Q}' \int \hat{Q} \int \hat{Q} \int \hat{Q} \dots,$$

- ▶ The so-called \hat{Q} -box is a collection of irreducible valence-linked diagrams
- ▶ The integral sign represents a generalized folding operation

The renormalization of the NN potential

Nowadays there are **two approaches** to the renormalization of the short-range correlations:



The renormalization of the NN potential

Nowadays there are **two approaches** to the renormalization of the short-range correlations:

- ▶ to renormalize the V_{NN} integrating out the high-momentum components of the potential - $V_{\text{low-}k}$ or **SRG approaches**
- ▶ to resort to realistic potential derived from the **chiral perturbation theory** and defined only for momenta below a cutoff Λ

The renormalization of the NN potential

Both ways are rooted in the **EFT**, providing a suitable way to deal with **meson theory** and **QCD**, respectively

The renormalization of the NN potential

Both ways are rooted in the **EFT**, providing a suitable way to deal with **meson theory** and **QCD**, respectively

Both pictures need to include **many-body terms**, aside the **2NF**

The renormalization of the NN potential

Both ways are rooted in the **EFT**, providing a suitable way to deal with **meson theory** and **QCD**, respectively

Both pictures need to include **many-body terms**, aside the **2NF**

Many-body forces recover what has been left out when constructing a **nucleon-nucleon** potential below a certain energy scale

Low-momentum nucleon-nucleon potentials: $V_{\text{low-k}}$

Inspiration to renormalize V_{NN} :

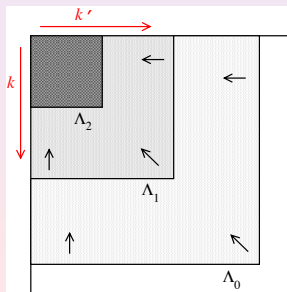
- ▶ Effective field theory (EFT)
- ▶ Renormalization group (RG)

Low-momentum nucleon-nucleon potentials: $V_{\text{low}-k}$

Inspiration to renormalize V_{NN} :

- ▶ Effective field theory (EFT)
- ▶ Renormalization group (RG)

from EFT: we restrict the configurations of $V_{NN}(k, k')$ to those with $k, k' < k_{\text{cutoff}} = \Lambda$



- ▶ Input V_{NN} : $V_{\text{low-k}}$ derived from the high-precision NN CD-Bonn potential with two different cutoffs: $\Lambda = 2.1, 2.6 \text{ fm}^{-1}$.
- ▶ H_{eff} obtained calculating the Q -box up to the 3rd order in $V_{\text{low-k}}$.
- ▶ Model spaces:
 - ▶ For protons: $0g_{7/2}, 1d_{5/2}, 1d_{3/2}, 2s_{1/2}, 0h_{1/2}$
 - ▶ For neutrons: $0h_{9/2}, 1f_{7/2}, 1f_{5/2}, 2p_{3/2}, 2p_{1/2}, 0i_{13/2}$
- ▶ Single-particle energies are taken from the experiment: this will help to stress the role played by $3NF$ forces on the two-body residual interaction

LETTER

doi:10.1038/nature12426

Masses of exotic calcium isotopes pin down nuclear forces

F. Wienholtz¹, D. Beck¹, K. Blaum¹, Ch. Bregmann¹, M. Brennerhöfer¹, R. E. Cañales^{1,2}, S. Geoghegan¹, J. Harber¹, J. D. Holt^{3,4}, M. Kowarik¹, S. Krein¹, J. D. Larmann¹, V. M. Máté¹, J. Mennendörfer¹, D. Neuhöfer¹, M. Rosenbusch¹, L. Schwikowski¹, A. Schwab¹, J. Simons¹, J. Stenpeit¹, R. W. Wülfel¹ & K. Zuber¹

The properties of exotic nuclei on the verge of existence play a fundamental part in our understanding of nuclear interactions¹. Exotically neutron-rich nuclei become sensitive to one aspect of nuclear forces². Calcium, with its doubly magic isotopes ⁴⁰Ca and ⁴⁸Ca, is an ideal test for nuclear shell evolution, from the safety of stability to the limits of existence. With a closed proton shell, the calcium isotopes mark the frontier for calculations with three-nucleon forces from chiral effective field theory³. Whereas predictions for the masses of ⁴⁰Ca and ⁴⁸Ca have been validated by direct measurements⁴, it is an open question as to how nuclear masses evolve for heavier calcium isotopes. Here we report the mass determination of the exotic calcium isotopes ⁴²Ca and ⁴⁴Ca, using the multi-reflexion time-of-flight mass spectrometer⁵ of ISOLTRAP at CERN. The measured masses unambiguously establish a present shell closure at neutron number *N* = 32, in excellent agreement with our theoretical calculations. This results increase our understanding of neutron-rich matter and pin down the subtle components of nuclear forces that are at the forefront of theoretical developments constrained by quantum chromodynamics⁶.

Infinite nuclei with extreme neutron-to-proton asymmetries exhibit shell structures generated by unpaired nucleons of shell occupation. Their description poses enormous challenges, because most theoretical models have been developed for nuclei at the valley of stability. It is thus an open question how well they can predict new magic numbers emerging far from stability^{7,8}. This is doubly helpful to our understanding of the different components of the strong force between neutrons and protons (spin-orbit and tensor interactions), which modify the gaps between single-particle orbits⁹, and of three-body forces, which are present in all nucleon–nucleon and neutron–rich system based on nuclear forces¹⁰. The resulting magic numbers, as well as the strength of the corresponding shell gaps, are critical for global predictions of the nuclear landscape^{11,12}, and thus for the successful modelling of matter in astrophysical environments. Three-body forces arise naturally in chiral effective field theory¹³, which provides a systematic basis for nuclear forces connected via an expansion to the underlying theory of quarks and gluons, namely quantum chromodynamics. Owing to the constant decrease of

effective field theory, there are only two unmodelled low-energy couplings in chiral three-nucleon forces for leading and sub-leading orders. These are constrained by the properties of light nuclei ¹⁴ and ¹⁵ and ¹⁶, so that all heavier elements are predicted in chiral effective field theory. The present frontier of three-nucleon forces is located in the calcium isotopes, where the structure evolution is dominated by valence neutrons due to the closed proton shell at atomic number *Z* = 20 (ref. 15). This prediction withstands a recent challenge from direct Penning trap mass measurements of ⁴⁰Ca and ⁴⁸Ca at TITANTRAP¹⁷, which have established a substantial change from the previous mass evaluation and have completely open how nuclear masses evolve past ⁴⁸Ca. This region is also very exciting because of evidence of a new magic neutron number *N* = 32 from nuclear spectroscopy^{18,19}, with a high *Z* excitations energy in ⁴²Ca (ref. 19, 20). These results are accompanied by successful theoretical studies based on phenomenological shell model interactions^{20,21}, which are similar for the excitation spectra at *N* = 32 but disagree markedly in their predictions for ⁴⁴Ca and further away from stability. Here we present the first mass measurements of the exotic calcium isotopes, and unambiguously establish a strong shell closure, in excellent agreement with the predictions including three-nucleon forces.

The mass of a nucleus provides direct access to the binding energy, the net result of all interactions between nucleons. Penning traps prove to be the method of choice when it comes to high-precision mass determination of exotic nuclei²². The mass in an ion trap is measured with charge *q* stored in a magnetic field *B* and compensated by cyclotron frequency $\nu_c = q\hbar/2\pi m$, that of a well-known reference nucleus ν_{ref} . The frequency ratio $\nu_c/\nu_{ref} = m_{ref}/m$ (cyclotron resonance) then yields the mass *m* directly and thus, to the greatest extent of the setup.

We have made a critical step towards determining the precise calcium masses by introducing a new method of precision mass spectrometry for short-lived nuclei. The development and measurements were performed with ISOLTRAP²³, a high-resolution Penning-trap mass spectrometer at the ISOLDE/CERN facility. This method was used to confirm and even improve the accuracy of the recent mass measurements

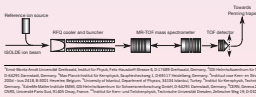


Figure 1 Experimental set-up. Main components relevant for the study involving ISOLTRAP and the reference ion source, multi-reflexion time-of-flight (MR-TOF) mass spectrometer and TOF analyzer to determine the absolute time-of-flight time of the ions.

¹ Fritz-Haber Laboratory, Berlin, Germany; ² Physikalisches Institut, Universität Bonn, Germany; ³ Institut für Experimentelle Kernphysik, Universität Wien, Austria; ⁴ Institut für Experimentelle Kernphysik, Universität Wien, Austria; ⁵ Institut für Experimentelle Kernphysik, Universität Wien, Austria; ⁶ Institut für Experimentelle Kernphysik, Universität Wien, Austria; ⁷ Institut für Experimentelle Kernphysik, Universität Wien, Austria; ⁸ Institut für Experimentelle Kernphysik, Universität Wien, Austria; ⁹ Institut für Experimentelle Kernphysik, Universität Wien, Austria; ¹⁰ Institut für Experimentelle Kernphysik, Universität Wien, Austria; ¹¹ Institut für Experimentelle Kernphysik, Universität Wien, Austria; ¹² Institut für Experimentelle Kernphysik, Universität Wien, Austria; ¹³ Institut für Experimentelle Kernphysik, Universität Wien, Austria; ¹⁴ Institut für Experimentelle Kernphysik, Universität Wien, Austria; ¹⁵ Institut für Experimentelle Kernphysik, Universität Wien, Austria; ¹⁶ Institut für Experimentelle Kernphysik, Universität Wien, Austria; ¹⁷ Institut für Experimentelle Kernphysik, Universität Wien, Austria; ¹⁸ Institut für Experimentelle Kernphysik, Universität Wien, Austria; ¹⁹ Institut für Experimentelle Kernphysik, Universität Wien, Austria; ²⁰ Institut für Experimentelle Kernphysik, Universität Wien, Austria; ²¹ Institut für Experimentelle Kernphysik, Universität Wien, Austria; ²² Institut für Experimentelle Kernphysik, Universität Wien, Austria; ²³ Institut für Experimentelle Kernphysik, Universität Wien, Austria.

LETTER

doi:10.1038/nature12422

Evidence for a new nuclear ‘magic number’ from the level structure of ⁵⁴Ca

D. Sappensbach¹, S. Takahashi¹, N. Aoi¹, P. Doornik¹, M. Mitsuhashi¹, H. Wang¹, H. Rahn¹, N. Fukuda¹, S. Gei¹, M. Homma¹, J. Lee¹, K. Maruyama¹, S. Michimasa¹, M. Motoyoshi¹, D. Nishimura¹, T. Otsuka¹, H. Sakurai¹, Y. Shiga¹, P. A. Söderström¹, T. Sumikama¹, H. Suzuki¹, R. Taniuchi¹, Y. Utsuno¹, J. J. Valiente¹ & K. Yoshida¹

Atomic nuclei are finite quantum systems composed of two distinct types of fermion—protons and neutrons. In a manner similar to that of electrons orbiting in an atom, protons and neutrons in a nucleus form shell structures. In the case of stable, naturally occurring nuclei, large energy gaps exist between shells that fill completely when the proton or neutron number is equal to 2, 8, 20, 28, 50, 82 or 126 (ref. 1). Away from stability, however, these so-called ‘magic numbers’ are known to evolve in systems with a large imbalance of protons and neutrons. Although some of the standard shell closures can disappear, new ones are known to appear². Studies aiming to identify and understand such behaviour are of major importance in the field of experimental and theoretical nuclear physics. Here we report a spectroscopic study of the neutron-rich nucleus ⁵⁴Ca in its lowest ground state of 20 protons and 34 neutrons using proton knockout reactions to find radioactive progenies. The results highlight the doubly magic nature of ⁵⁴Ca and provide direct experimental evidence for the onset of a stable subshell closure at neutron number 34 for neutrons far from stability.

The shell structure of the atomic nucleus was first successfully described more than 60 years ago³. However, the question of how robust the standard magic numbers are in unstable nuclei with a large excess of neutrons—often referred to as ‘exotic’ nuclei—has been one of the main driving forces behind nuclear structure studies that focus on changes to the shell structure, called ‘shell evolution’⁴. A noteworthy example is the disappearance of the *N* = 20 (neutron number 10) standard magic number (ref. 4), a nucleus that deviates from the stable isotopes in the Segre chart. On the contrary, exotic oxygen nuclei provide evidence for the onset of a new magic number *N* = 16, one that is not observed in stable nuclei. In both cases, the tensor force, a non-central component of the nuclear force, has a key role in describing the emergence of *N* = 16^{5,6}.

The origin of the shell chart around exotic calcium isotopes has also contributed valuable input to what is predicted from mass measurements over recent years using state-of-the-art nuclear models. Enhanced excitation energies of first *π*[−] *ν*² states (spin, parity, *J*) and reduced *ν* *ν* transition probabilities, which are indicators of nuclear shell gaps, for ⁴²Ca (ref. 6, 7), ⁴⁴Ca (ref. 8) and ⁴⁶Ca (ref. 10, 11) provide substantial evidence for the onset of a stable energy gap at *N* = 32. This result was recently confirmed by the first *π*[−] *ν*² ground-state transition in neutron-rich Ca isotopes⁹. In the framework of tensor-force-driven shell evolution¹², the *N* = 32 subshell closure is directly connected to the weakening of the attractive nucleon–neutron interaction between protons (π) and neutrons (ν) in the *ν*_{1/2} and *ν*_{3/2} single-particle orbits (SPO) as the number of protons in the SPO is reduced and the magnitude of the *π*_{1/2}–*ν*_{1/2} energy gap increases (Fig. 1a–c).

It is well established that the *N* = 32 subshell closure is recent years in either or not the onset of another subshell gap occurs in exotic nuclei.

N = 34 isotopes, which was suggested qualitatively more than a decade ago¹³ on the basis of the general properties of nuclear forces. The onset of an appreciable subshell closure at *N* = 34 is illustrated in Fig. 1d, indicating an energy gap between the *ν*_{1/2} and *ν*_{3/2} SPOs in ⁵⁴Ca that is comparable to the separation of the *ν*_{1/2} and *ν*_{3/2} spin-orbit partners, which is also implied by recent theoretical results; see, for example, ref. 14. We note, however, that no *N* = 34 subshell closure was reported in the experimental investigations of ⁷¹Ca (ref. 13) or ⁷²Ca (ref. 11, 16), and notable drops on this magic number for Ca isotopes has been raised¹⁷. Indeed, as indicated in Fig. 2a, theoretical predictions of the energy of the first *π*[−] *ν*² state for ⁵⁴Ca vary considerably, ranging from ~1 MeV in some cases to as high as ~4 MeV in others^{18,19}, despite exhibiting clear agreement for lighter isotopes; for example, the prediction of the same transition to within only 0.4 MeV of the empirical result for ⁵⁰Ca. Such stark discrepancies in *N* = 34 reflect the need for direct experimental input on the matter.

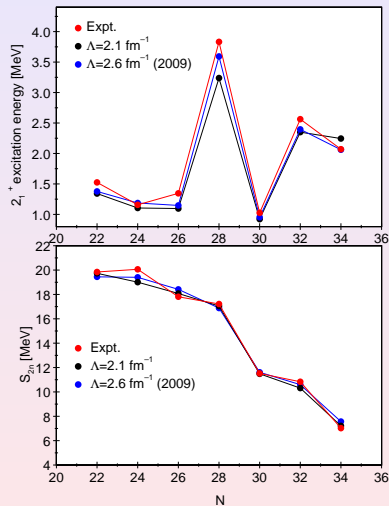
To address this issue, we report on an experimental study of ⁵⁴Ca to clarify the strength of the *N* = 34 subshell gap in nuclei far from stability. The energies of nuclear excited states were investigated using proton knockout reactions involving ⁵⁶Ca and ⁵⁷Ca projectiles on a ²⁰Ne target at the Radioactive Isotope Beam Factory, Japan, operated by the RIKEN Nishina Center and the Center for Nuclear Study, University of Tokyo. Experimental details are provided in Methods Summary. Particle identification plots indicating the radioactive species were produced through the BigRIPS separator and ZeroDegree spectrometer²⁰, which were used to select and tag radioactive beam components and neutron progenies, are presented in Fig. 2a and Fig. 3b, respectively. We note that the spin-parity of the ground state of ⁵⁴Ca, which was critical to the success of the experiment, is unique to the Radioactive Isotope Beam Factory. Excited-state energies were deduced solely by applying the techniques of *in-beam* *ν*² spectroscopy.

The *ν*² rays measured in coincidence with ⁵⁴Ca projectile production through the first *π*[−] *ν*² and *π*[−] *ν*³ transitions are presented in Fig. 4a. The *ν*² rays were corrected in the laboratory frame of reference have been verified for Doppler shifts, and as the transitions appear at the energies they would in the rest frame of the nucleus. The most intense *ν*² ray line in the ⁵⁴Ca spectrum, the peak at 2.04(10) keV (ref. 1, 2) in Fig. 4a, is assigned as the transition from the first *π*[−] state (2[−]) to the *ν*² ground state. An additional *ν*² transition are located at 1.65(10) keV, and, respectively, 1.18(21) keV (Fig. 4b) above a *ν*² transition observed with the condition of a prompt coincidence (c(10) ns) with the 2.04(10) keV ray, indicating that the weaker transitions were emitted in decay sequences involving the 2[−] *ν*² ground-state transition. On the basis of the *ν*² transition energies, the 1.65(10)-keV transition is proposed to depopulate a level *K* = 4 question that has been raised¹⁷ and is recent years in right section of Fig. 4a. Placement of the 1.18(21)-keV transition in the

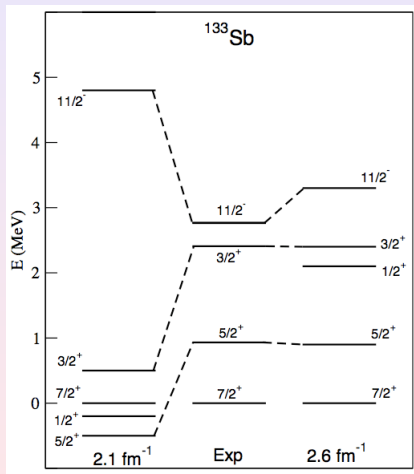
¹ Fritz-Haber Laboratory, Berlin, Germany; ² Physikalisches Institut, Universität Bonn, Germany; ³ Institut für Experimentelle Kernphysik, Universität Wien, Austria; ⁴ Institut für Experimentelle Kernphysik, Universität Wien, Austria; ⁵ Institut für Experimentelle Kernphysik, Universität Wien, Austria; ⁶ Institut für Experimentelle Kernphysik, Universität Wien, Austria; ⁷ Institut für Experimentelle Kernphysik, Universität Wien, Austria; ⁸ Institut für Experimentelle Kernphysik, Universität Wien, Austria; ⁹ Institut für Experimentelle Kernphysik, Universität Wien, Austria; ¹⁰ Institut für Experimentelle Kernphysik, Universität Wien, Austria; ¹¹ Institut für Experimentelle Kernphysik, Universität Wien, Austria; ¹² Institut für Experimentelle Kernphysik, Universität Wien, Austria; ¹³ Institut für Experimentelle Kernphysik, Universität Wien, Austria; ¹⁴ Institut für Experimentelle Kernphysik, Universität Wien, Austria; ¹⁵ Institut für Experimentelle Kernphysik, Universität Wien, Austria; ¹⁶ Institut für Experimentelle Kernphysik, Universität Wien, Austria; ¹⁷ Institut für Experimentelle Kernphysik, Universität Wien, Austria; ¹⁸ Institut für Experimentelle Kernphysik, Universität Wien, Austria; ¹⁹ Institut für Experimentelle Kernphysik, Universität Wien, Austria; ²⁰ Institut für Experimentelle Kernphysik, Universität Wien, Austria.



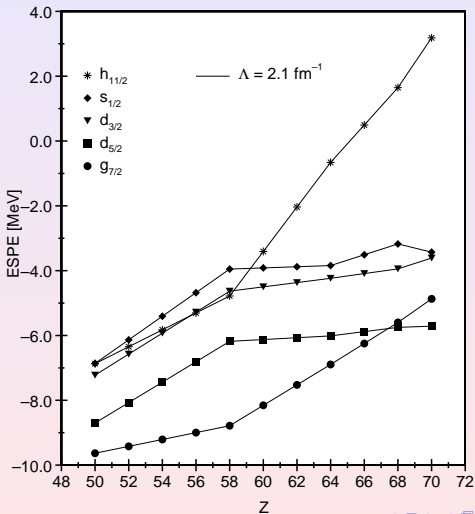
Results for the calcium isotopes



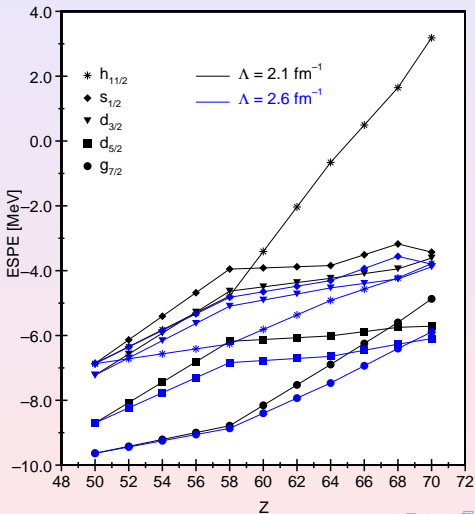
Single-particle states in ^{133}Sb



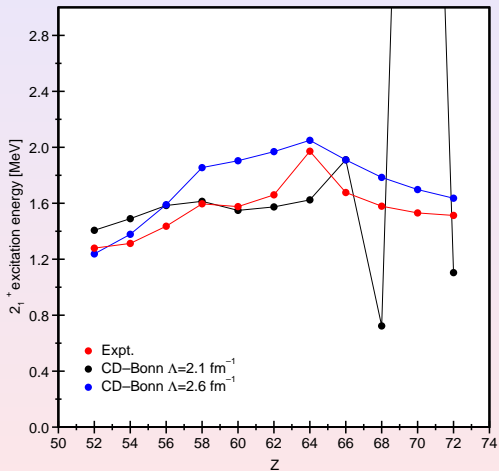
Effective single-particle energies of N=82 isotones



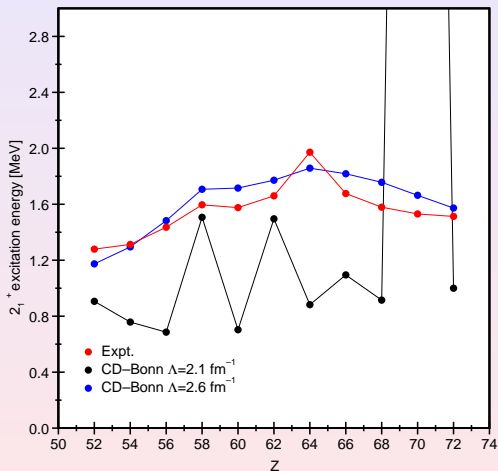
Effective single-particle energies of N=82 isotones



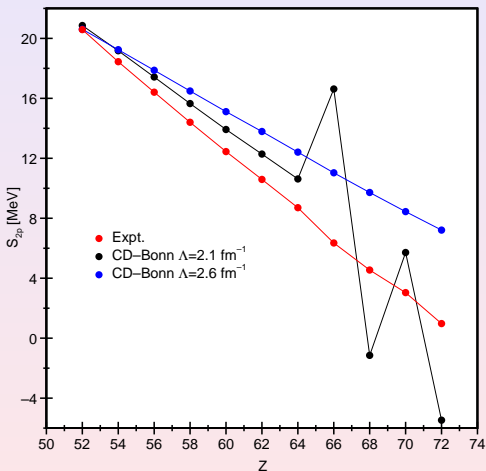
2_1^+ energies in N=82 isotones



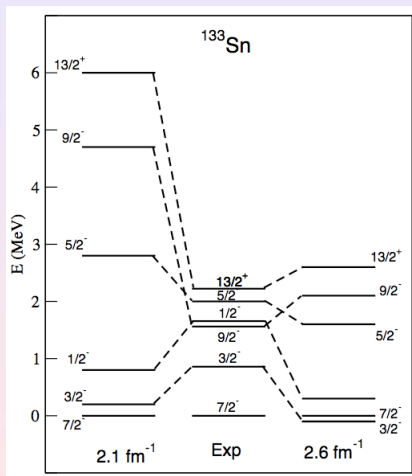
2_1^+ energies in N=82 isotones: theoretical s.p.e.



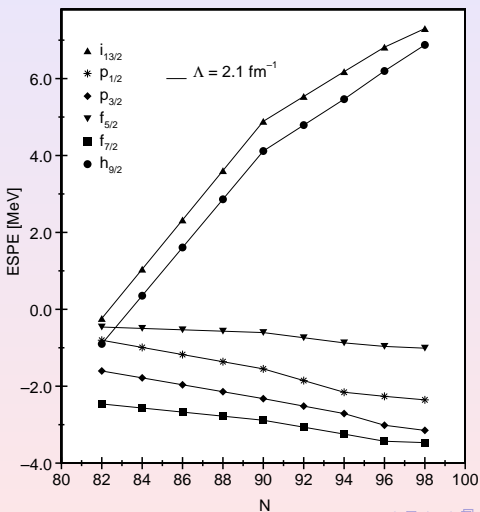
Two-proton separation energies of N=82 isotones



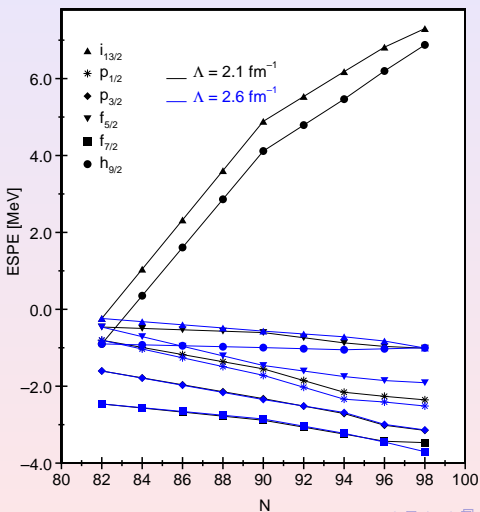
Single-particle states in ^{133}Sn



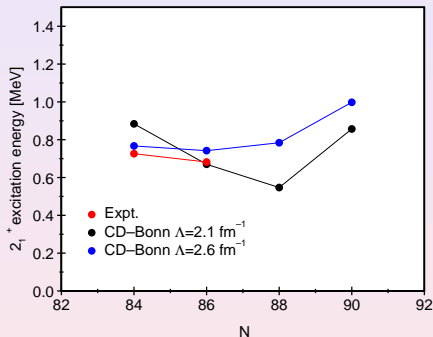
Effective single-particle energies of tin heavy isotopes



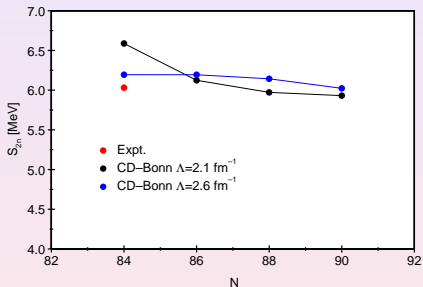
Effective single-particle energies of tin heavy isotopes



2_1^+ energies in heavy tin isotopes



Two-neutron separation energies of heavy tin isotopes



Cutoff (in fm^{-1})	P_D (in %)
2.1	3.96
2.6	4.49
∞	4.85

Summary

- ▶ **Monopole components** of the shell-model hamiltonian are affected by the lack of the inclusion of **3NF**
- ▶ This seems to be far less important for model spaces built up by **full HO major shells**
- ▶ In nuclei above ^{132}Sn **nucleon-nucleon** potentials with a **larger** cutoff may reduce the role played by **3NF**
- ▶ The latter effect is probably connected to the **tensor component** of the input **nucleon-nucleon** potential